Eidgenössische Technische Hochschule Zürich
Swiss Federal Institute of Technology Zurich

innovative composite structures

Development of a Low-Cost Modal Analysis System

Roman Rüttimann

Master Thesis

Nino Ceresa
Prof. Konrad Wegener

Institute of Machine Tools and Manufacturing

Abstract

Experimental modal analysis in tandem with the modal model of a machine tool is a powerful tool for the evaluation of the machine tools' dynamic behavior. But because experimental modal analysis is an expensive procedure, both due to high instrument costs and the need for experienced operators, the modal model is often not verified.

With the aim to decrease instrument costs and increase the use of experimental modal analysis, the system presented in this thesis consists of a micro controller based data acquisition system, a modal impact hammer and a low-cost accelerometer. The latter is a capacitive micro-electro-mechanical-sensor and the impact hammer is using a strain gauge load cell as impact sensor.

For the implementation of a low-cost modal analysis system based on the aforementioned components a micro controller based bus system and a specialized communication protocol is suggested.

Zusammenfassung

Die experimentelle Modalanalyse, in Kombination mit dem modalen Modell einer Werkzeugmaschine, ist ein mächtiges Werkzeug, um das dynamische Verhalten der Werkzeugmaschine zu evaluieren. Teure Messinstrumente und der Bedarf an erfahrenen Bedienern machen die experimentelle Modalanalyse allerdings zu einem kostspieligen Unterfangen. Oft wird daher das modale Modell gar nicht validiert.

Mit dem Ziel die Kosten für Messinstrumente zu senken und den Gebrauch von experimenteller Modalanalyse zu steigern, wird in dieser Arbeit ein System vorgestellt, welches aus einem Mikrokontroller-basierten Datenakquisitionssystem, einem Impulshammer und einem kostengünstigen Beschleunigungssensor besteht. Letzterer ist ein kapazitiver mikro-elektro-mechanischer Senor und der Impulshammer ist mit einer Dehnmessstreifen basierten Ladungszelle ausgestattet.

Für die Umsetzung eines kostengünstigen Modalanalysesystems auf der Grundlage der zuvor genannten Komponenten, wird ein Mikrokontroller-basiertes Bus-System mit einem spezialisierten Kommunikationsprotokoll vorgeschlagen.

Entwicklung eines Low-cost-Modalanalyse-Systems

Bachelor- / Masterarbeit

Problemstellung

Mit zunehmender Verbreitung von simulationsgestützer Entwicklung wird auch der Bedarf nach Methoden zur Modellverfikation in der Industrie grösser. Die experimentelle Modalanylse (EMA) ist ein mächtiges Werkzeug zur Validierung von Simulationsmodellen von Werkzeugmaschinen. Dabei wird die Struktur mittels Impulshammer angeregt und die Antwort mit Beschleunigungssensoren gemessen. Kommerziell erhältliche EMA-Systeme kosten jedoch schnell über 50‘000 CHF und sind daher für die breite Anwendung nicht geeignet. Für die Modellvalidierung sind jedoch die Auflösung und die Abtastrate des Messsystems häufig weniger kritisch, was den Einsatz von günstigeren Komponenten zulassen würde.
Mit den heute erhältlichen MEMS-Beschleunigungssensoren (wie sie in jedem Smartphone verbaut werden) und Mikrocontroller-Plattformen (wie Arduino) ergibt sich die Möglichkeit, ein einfaches EMA-System aus sehr günstigen Komponenten zu entwickeln.

Aufgabenstellung

Auf Basis von günstigen Sensoren und Mikrokontrollern, sowie freier open-source Software, soll ein preiswertes Messsystem zur Validierung von Simulationsmodellen entwickelt werden.

Arbeitspakete:

- Festlegen der Anforderungen an das Messsystem
- Auswahl der Komponenten
- Entwicklung der Software zum Auslesen der Sensoren (Arduino)
- Evaluation der Auswertesoftware (open-source)
- Vergleich mit einem komerziellen EMA-System
- Präsentation der Ergebnisse und Diskussion

Aufteilung der Arbeit: 70% Entwicklung/Programmierung, 20% Messen, 10% Bericht

Anforderungen: Erfahrung mit Programmierung; optimalerweise im Bereich Mikrokontroller (Arduino).

Kontakt:

Nino Ceresa PFA E 82 044 633 37 19 ceresa@inspire.ethz.ch

Contents

List of Abbreviations

AAF	Anti Aliasing Filter
AMP	Amplifier
ADC	Analog to Digital Converter
ASCII	American Standard Code For Information Interchange
CPU	Central Processing Unit
DAC	Data Acquisition
EMA	Experimental Modal Analysis
FIFO	First In, First Out
FPGA	Field Programmable Gate Array
FRF	Frequency Response Function
MCU	Microcontroller Unit
MEMS	Micro-Electro-Mechanical-Systems
MT	Machine Tools
LC	Load Cell
LPF	Low Pass Filter
OP-AMP	Operational Amplifier
IN-AMP	Instrumentation Amplifier
IC	Integrated Circuit
RS	Recommended Standard
SPI	Serial Peripheral Interface
USB	Universal Serial Bus

1

Introduction

1.1 Motivation

The Experimental Modal Analysis (EMA) is a powerful tool for evaluating dynamic models of structures. Despite its extensive usage in the aerospace industry, in many other engineering fields the benefits of EMA are overshadowed by the initial investment and the operator costs of an EMA system. To enable Machine Tools (MT) manufactures to test their products and validate their modal predictions. Progress in Micro-Electro-Mechanical-Systems (MEMS) technology enables the use of new generation of low-cost senors in EMA.

1.2 Related Work

Considering the use of low-cost accelerometers in EMA specifically, a two-point vibration measurement system with a bandwidth of 500 Hz has been developed [2]. The authors Chan and Huang used this system to conduct a multiple-point vibration test a MT. Operating at lower frequencies, Beskhyroun and Ma used MEMS based accelerometers to conduct an EMA on building structures. Piana et al. developed a modal test system, which uses piezoelectric transducers that are typically used to tune musical instruments as response sensors [6]. Moreover, a construction kit for a low-cost vibration analysis system was proposed by Vollmer et al. back in 2009 [10].

In the field of civil engineering, bridges and skyscrapers require continuous vibration signal logging for structural health monitoring. This leads to an increased interest in driving down the cost of accelerometer based vibration monitoring systems. Girolami et al. has developed a low-cost MEMS systems for structural health monitoring of civil structures [5].

Structural health monitoring is also required in rotary systems such as gas and wind turbines. Esu et al. integrated low-cost accelerometers in wind turbines and logged data via radio frequency to a central device.

Addressing low-cost impact hammer constructions, Waltham and Kotlicki implemented a piezoelectric transducer in a hammer, that is designed to trigger barbecue lighters [11]. And for inexpensive calibration of a load cell used for modal testing, Wang et al. introduced practical techniques [12].

1.3 Overview

First fundamentals in measurement instrumentation, sensors and EMA is introduced in the state of the art. Then the Data Acquisition (DAC) developed for this project is presented in chapter 3. Testing environment are described in the chapter 4 and measurement results are discussed in results. Finally the conclusion gives reflects on the project.

2

State of the Art

2.1 Measurement

The process of measurement is the comparison of data from the physical world in the frame of an agreed standard. It is carried out by using an instrument.

This section points to some key aspects of measurement instruments and components, used in the frame of this thesis. As a result some sections of [13] are summarized.

2.1.1 Measurement and Instrumentation

Measurement instruments translate signals from the physical world into an agreed upon standard. These standardized signals can be compared, altered and stored. The original data acquired from the physical signal is usually in analog form. This is then converted to digital before it is passed on. The signal chain of a typical digital measurement instrument is shown in Figure 2.1.

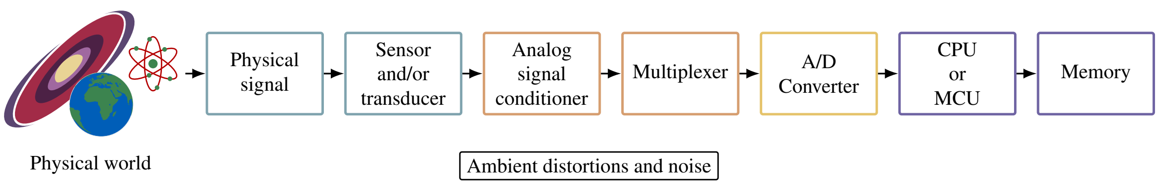

Figure 2.1: *Digital measurement instrument*

2.1.2 Sensors and Transducers

A device that responds to a changing phenomenon is called sensor. If we need to transfer the energy from one to another, we use a device called transducer. If one compares sensors and transducers based on the energy input and output, one identifies three types:

- In *modifiers* a specific energy form is not converted but modified. Hence they use the same form of energy as input and output.
- *Self-generators* give out electric signals from non-electric inputs without the need of additional energy.
- *Modulators* in contrast give out electric signals from non-electric inputs, but require an additional energy input.

As part of this we focus on self-generating piezoelectric sensors, capacitive modulators that convert mechanical deformation in a static electric field into an electric current, as well as strain gauge based modulators.

2.1.3 Load Cells

A force measurement sensor that converts a force into an electrical signal is called Load Cell (LC). The basis of force measurement results from the physical behavior of a body under external forces. Depending on the bandwidth and magnitude of the signal, as well as the duration of the signal capture, different methods of force measurement are applied in various designs. The methods in brief are:

- Balancing the unknown force against a standard mass through a system of levers
- Measuring the acceleration of a known mass
- Equalizing it to a magnetic force generated by the interaction of a current-carrying coil and a magnet
- Distributing the force on a specific area and then measuring the pressure
- Converting the applied force into the deformation of an elastic element

Furthermore, these methods yield numerous of designs of measuring equipment. Each of which addressing two main problems. First, the physical and geometrical constrains by the application of the device and second, the means by which the force can be converted into an electrical signal.

LCs in EMA equipment designs typically use piezoelectric sensors because of their high bandwidth in compact designs and their capability to detect small deflections.

2.1.4 Accelerometers

Accelerometers are sensors that convert acceleration into an electrical signal. In order to measure a physical phenomenon we use seismic masses that act on the sensor structure based on their inertia properties. In strain gauge based accelerometers the structure translates the inertia force into a deformation, where capacitive sensor structures may use deformations or relative motions of separate components in an electric field. In piezoelectric accelerometers the seismic mass deforms a piezoelectric material, see Figure 2.2.

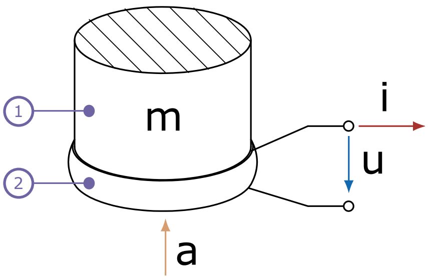

Figure 2.2: *Function principle of a piezoelectric accelerometer*

a	:	Acceleration
m	:	Mass
i	:	Induced Current
u	:	Induced voltage
1	:	Seismic mass
2	:	Piezoelectric material

Table 2.1: *Legend to Figure 2.2*

In seismic accelerometers the base of the arrangement is motion. When describing the one dimensional case, one can express non-stationary random vibrations acting on the accelerometer as

$$m\frac{\mathrm{d}^2 z}{\mathrm{d}t^2} = c\frac{\mathrm{d}z}{\mathrm{d}t} + kz = mg\cos(\theta) - m\frac{\mathrm{d}^2 x_1}{\mathrm{d}t^2} \tag{2.1}$$

where

m is the seismic mass
$z = x_2 - x_1$ is the relative motion between the mass and the base
x_1 is the displacement of the base
x_2 is the displacement of the mass
θ is the angle between sense axis and gravity

The second-order system expressed in Laplace transform thus takes the form

$$G(s) = \frac{X(s)}{F(s)}\frac{K}{s^2/\omega_n^2 + 2\zeta s/\omega_n + 1} \tag{2.2}$$

where

s is the Laplace operator
$K = 1/k$ is the static sensitivity
$\omega_n = \sqrt{k/m}$ is the undamped frequency in $\mathrm{rad/s}$
$\zeta = c/2\sqrt{km}$ is the damping ratio

It is obvious that the performance of accelerometers depends on their static sensitivity, the natural frequency and the damping ratio. We want the accelerometer to have a linear transfer function in the range of operation. But namely the damping ratio can distort a measurement when operating an accelerometer near its eigenfrequency, see Figure 2.3.

2.1.5 Piezoelectric Sensors

Some materials develop electric charge proportional to directly applied mechanical stress. The same materials show the converse effect. A proportional strain of the material will occur to an applied electric field.

The first phenomenon has found its application in a variety of self-generating sensors that output electrical signals – namely in LCs and accelerometers, where the piezoelectric charge is converted into a current or voltage signal.

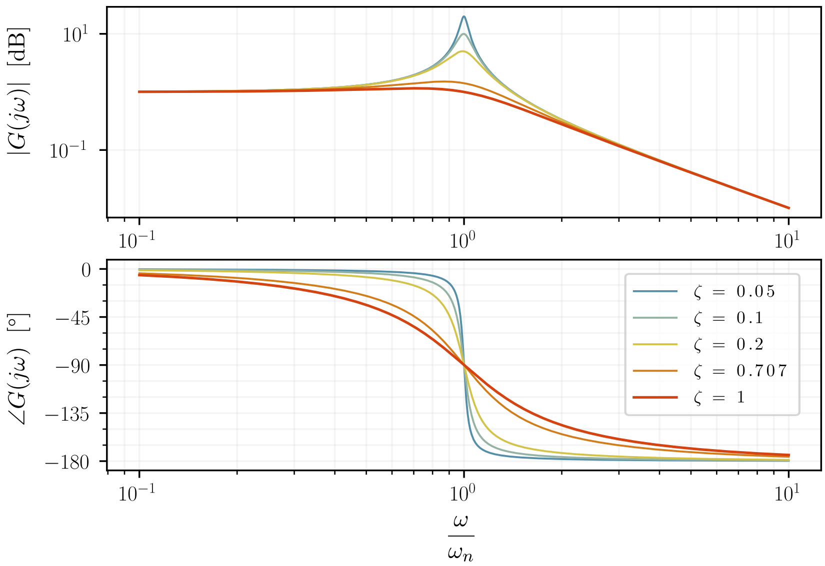

Figure 2.3: *Bode plots of second order system describing the dynamic behavior of seismic accelerometers*

Piezoelectric sensors are designed to exploit the piezoelectric effect of the material in one axis. Additionally, we use amplifier circuits so that the weak electrical signal, induced due to the piezoelectric charge, is elevated to amplitudes that are in the range of operation of standard electronic components. These circuits require additional energy. Commercially available LCs therefore require supplied energy – see Figure 2.4.

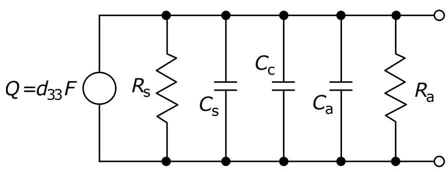

(a) *Piezoelectric sensor connected to a voltage amplifier*

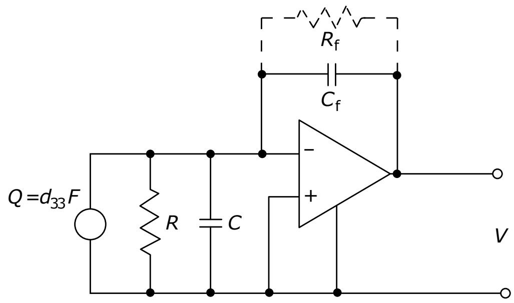

(b) *Strain gauge in Wheatstone bridge circuit*

Figure 2.4: *Piezoelectric sensors connected to amplifier circuits [13]*

Depending on the design of the sensor, piezoelectric materials are used in different shapes. Figure A.1 shows some possible variations.

2.1.6 Strain Gauge Load Cells

In strain gauge LCs the elastic properties of a material probe is exploited.

The probe is loaded in a controlled manner in its elastic region. Deformations are captured by a strain gauge at a suitable location. The probe deformation is directly determined by the force acting on the probe because of Hooke's law.

The strain gauges themselves each use a specific length gauge wire in order to reach a resistance of typically $120\,\Omega$. The wire is bonded between two thin sheets in coiled up form as can be seen in Figure 2.5a. The sheets act as insulating carrier and can be easily deformed with the intent of passing the load to the wire grid. The gauge is attached to the probe structure by a wax or a resin. The intent is that deformations in transversal direction of the strain gauge act on all coils simultaneously, changing their resistance. By using small sized strain gauges with respect to the probe, the mechanical and thermal properties of the strain gauge become negligible small. As an example, we assume the probe expands. Then a strain gauge on its surface experiences tension. The coils in the grid are therefore stretched and as a result of the generalized Hook's law the coil cross sections decrease. Both the strain in axial direction of the coil and the decreased coil cross sections increase the wire's resistance.

In order to measure deformations one needs to take environmental influences into consideration. It is well known that resistance is susceptible to variations in temperature. Placing the strain gauge in a wheatstone bridge, with resistors, that change their resistance in the same manner as the strain gauge will reduce the influence of temperature significantly – see Figure 2.5b.

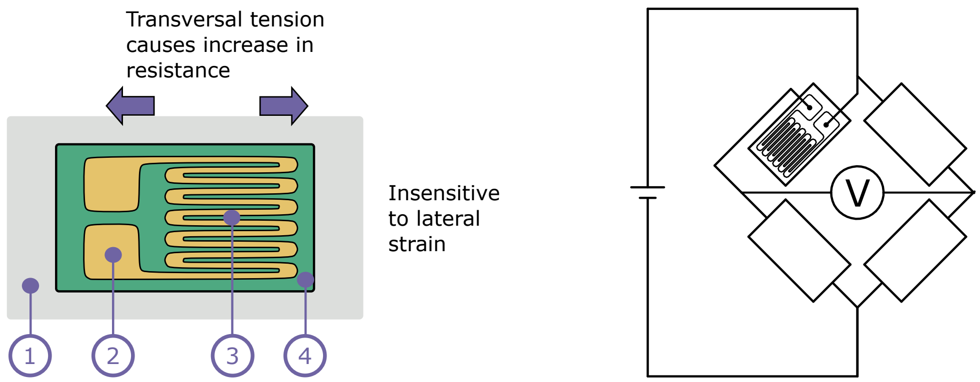

(a) *Strain gauge on structure, with (1) Structure, (2) Metal Pad, (3) Grid and (4) Carrier*

(b) *Strain gauge in Wheatstone bridge circuit*

Figure 2.5: *Strain gauge*

2.1.7 Capacitive Accelerometers

To understand the working principle of capacitive accelerometers, we first consider the displacement sensors.

Capacitive Displacement Sensors

The basic sensing element of a displacement sensor typically consists of two parallel electrodes with capacitance C.

$$C = f(d, A, \varepsilon) \tag{2.3}$$

With variable distance, dielectric material or area and with the measurement of the capacitance, we can then deduce the plate displacement in normal and parallel direction to the plates depending on the method used. See Figure 2.6

In variable displacement sensors, the distance between two capacitive plates is inversely proportional to the capacitance.

$$C(x) = \frac{\varepsilon A}{x} = \frac{\varepsilon_r \varepsilon_0 A}{x} \tag{2.4}$$

where

ε is dielectric constant or permittivity
ε_r is the relative dielectric constant (in air and vacuum $\varepsilon_r \approx 1$)
ε_0 is $8.854\,188\,\mathrm{F/m}$, the dielectric constant of vacuum
x is the distance of the plates in m
A is the effective area of the plates in m^2

In variable area displacement sensors, the capacitance is proportional to the reduction of area due to the movement of the plate.

$$C(x) = \frac{\varepsilon_r \varepsilon_0 (A - wx)}{d} \tag{2.5}$$

where

ε_2 is the permittivity of the displacing material (e.g. liquid)
w is the width
wx is the reduction in the area due to movement of the plate
d is the distance of the plates in m

In variable dielectric sensors, the capacitance depends on the ratio of each permittivity in the electric field.

$$C(x) = \varepsilon_0 w[\varepsilon_2 l - (\varepsilon_2 - \varepsilon_1)x] \tag{2.6}$$

$$\tag{2.7}$$

where

x is the displacement normal to the plate's direction
ε_1 is the relative permittivity of the dielectric material
ε_2 is the permittivity of the displacing material (e.g. liquid)

Differential capacitive displacement sensors are setup in capacitive arrangements that aim to eliminate nonlinearities. Different variations of these types of sensors exist. For example we can allow the outer plates to move and fix the middle one or we can reverse this setup. But the range is equal to twice the separation in both cases.

$$2\delta C = C_1 - C_2 = \frac{\varepsilon_r \varepsilon_0 lw}{d - \delta d} - \frac{\varepsilon_r \varepsilon_0 lw}{d + \delta d} = \frac{2\varepsilon_r \varepsilon_0 lwd}{d^2 + \delta d^2} \tag{2.8}$$

$$C_1 + C_2 = \frac{\varepsilon_r \varepsilon_0 lw}{d - \delta d} + \frac{\varepsilon_r \varepsilon_0 lw}{d + \delta d} = \frac{2\varepsilon_r \varepsilon_0 lwd}{d^2 + \delta d^2} \tag{2.9}$$

$$\tag{2.10}$$

Giving approximately

$$\frac{\delta C}{C} = \frac{\delta d}{d} \tag{2.11}$$

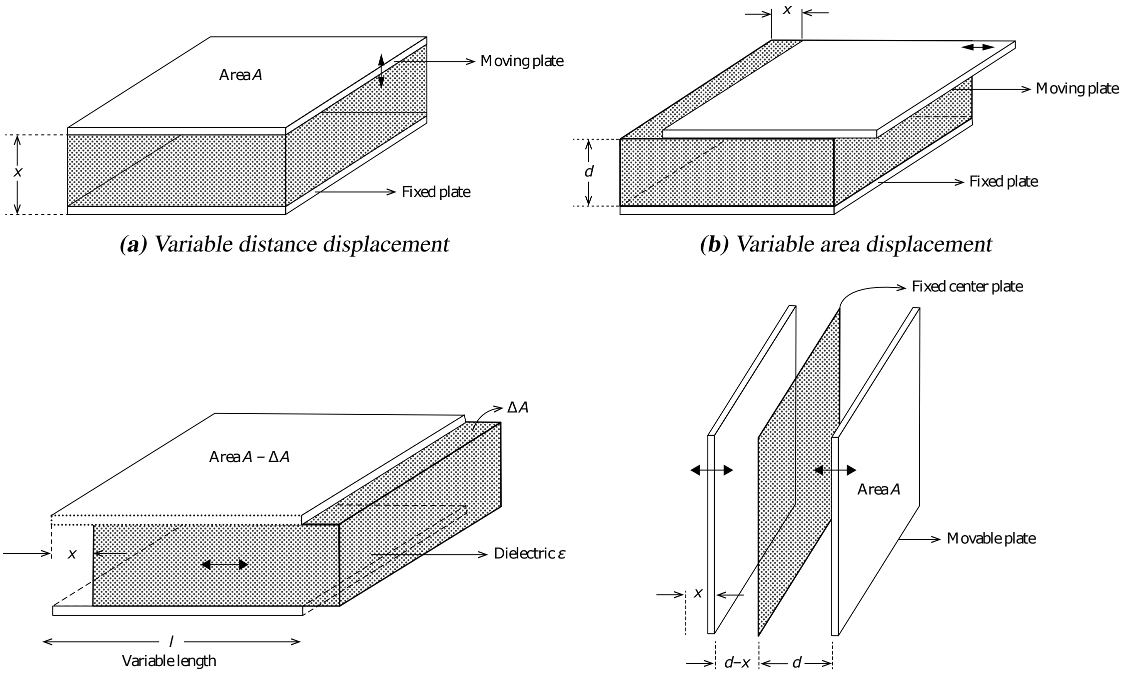

(a) *Variable distance displacement*

(b) *Variable area displacement*

(c) *Variable dielectric displacement*

(d) *Differential capacitive displacement*

Figure 2.6: *Capacitive displacement sensors [13]*

From Displacement to Acceleration

If one combines a capacitive displacement sensor with a seismic mass, one can use the inertia force to correlate the acceleration to the displacement and hence to the change in the electric field of the sensor. With the use of differential capacitive designs and high machining accuracy these designs can be realized in a tiny form factor as Micro-Electro-Mechanical-Systems (MEMS). A scheme of such a sensor is shown in Figure 2.7.

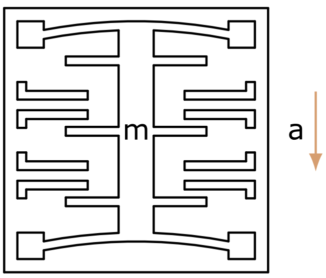

Figure 2.7: *Capacitive MEMS accelerometer, with acceleration a and the seismic mass m. The bridges attached to the seismic mass act as dielectricum.*

2.2 Signal Conditioning and Processing

In an ideal world, the signal output of a sensor would correlate to the measurand exactly. In real systems this is not the case because of a variety of reasons. In low-frequency applications, the most important ones are:

- The voltage or current rating at a sensor's output is not perfectly linear with respect to the measurand. Often the output is pseudo-linear in a limited range of values and deviates from the trajectory for values outside of this range.
- Noise and shifts introduced through the inherent impedances of analog components lead to deviations from the voltage or current rating of the sensor as well as deviations of these ratings with respect to the measurand itself.
- The quantization process causes the captured value space to have a finite resolution.
- Analog signals can only be digitized with a finite sampling rate. A discrete set of data points is captured instead of a continuous signal.

The field of signal processing includes analyzing, modifying and synthesizing signals. Most prominently, in data acquisition systems we convert analog signals to digital ones that can be further processed without the parasitic effects of the analog realm. On the opposite side when addressing these parasitic effects one needs to apply signal conditioning. In other words, before every processing step of an analog signal we need to consider signal conditioning. When dealing with digital signals, no signal conditioning is required.

2.3 Experimental Modal Analysis

EMA is a powerful tool to detect vibration related problems of mechanical structures. We use modes to characterize resonant vibrations of the system. This section is only a short excerpt of an introduction to EMA. An overview has been presented by Schwarz and Richardson in [7].

Vibration

In every vibration one can observe a combination of two different types of vibrations. The forced and the resonant ones. Forced vibrations in a structure are caused by

- Internally generated forces
- Unbalances
- External loads
- Ambient excitations

Common examples of vibration sources in MT are displayed in Figure 2.8.

Resonant vibration arises when one or more of the natural modes of vibration, inherent properties of the structure under investigation, is excited. Resonant vibration typically amplifies the vibration response to a level that exceeds deflection, stress and strain caused by static loading.

2.3.1 Frequency Response Measurement

In an EMA one needs to determine the Frequency Response Function (FRF) from input to output. To achieve this we measure the so called response or output function of the structure under investigation. The measurement instrument for this task uses a signal chain in form of 2.9.

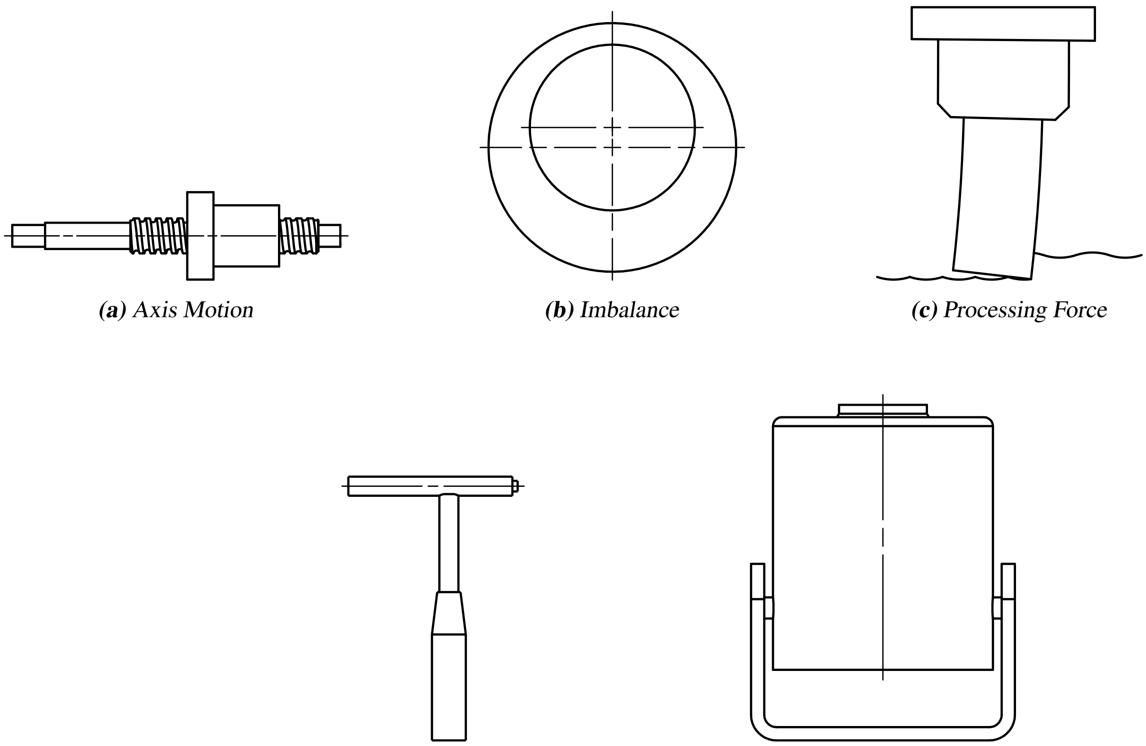

(a) Axis Motion *(b) Imbalance* *(c) Processing Force*

(d) Impact Hammer *(e) Modal Shaker*

Figure 2.8: *Sources of forced vibration. Note that (a), (b) and (c) occur during MT operation, while (d) and (e) are devices that are explicitly used for EMA to introduce vibrations into the structure of investigation.*

- The sensor on the structure translates the physical value (acceleration, velocity or position) into an electrical voltage or current, the analog signal variable.
- The amplifier amplifies the typically low power signal to fit it to the input range of the Analog to Digital Converter (ADC).
- The ADC samples and quantizes the analog signal. It is then converted into a digital signal, in which the quantity is expressed in form of a binary code.
- The discrete time signal is then stored on the computer memory.

[4]

2.4 Electronic Components

This section serves as an introduction to the function of selected electronic components and circuits. It does not give a complete overview of the state of the art. For more background on electronics [8] and [9] may be consulted.

Electronic components are divided into two main types; passive and active ones. Where active components are allowed to generate, amplify or oscillate an electrical signal, passive components can only absorb, dissipate or store electric energy.

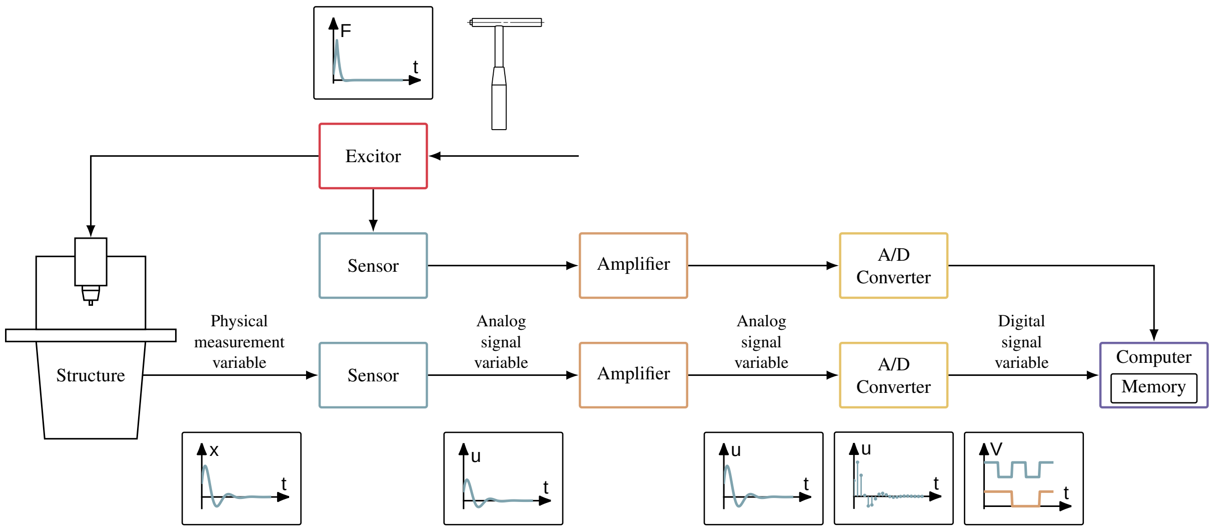

Figure 2.9: *FRF measurement setup*

2.4.1 Passive Components

Because of the increase in digital processing, the number of passive components has decreased drastically in modern electronic circuits. This, in addition to the trend of using more complex devices in favour to multiple simple passive components, has led to a great variety of passive components which are designed with emphasis on reliability.

Typical examples of passive components are:

Wires Depending on the mechanical requirements for the wire, it can either be designed with a solid core or a stranded wire core. A wire consisting of multiple smaller diameter conductors shows better flexibility but reduced current-carrying capacity at the same wire diameter. This is because of the smaller overall conductor cross-section of a stranded wire and, when transmitting high frequency signals, a greater power dissipation due to the more prevalent skin effect. Furthermore the simplicity of solid core wires makes them more resistant to corrosion and more suitable to be used in harsh environments.

Resistors Depending on the application different types of resistors can be applied. Fixed value resistors, can be used for safety of other components by dissipating heat or reducing to set the current and voltage in combination relative to other devices. Variable resistors change their value due to different physical phenomena. Thermistors show resistances that are highly susceptible to temperature changes, potentiometers resistance is manually tunable and photoresistors show a light dependant resistance, to name a few.

Capacitors Capacitors store energy in form of an electric field. They have many applications, most prominently in filter circuits and as bypass capacitors to reduce smooth out non constant power draws.

Inductive Devices Are devices that store energy in form of an electric field. In modern devices coils are less common due to benefits, when realizing the circuit with capacitors instead. But in specialized applications, namely when converting between electrical and mechanical signals, i.e. in motors, generators, loudspeakers etc.

2.4.2 Active Components

Active components show some form of amplification of the input signal in most cases; in other ones they generate vibrations, but generally an additional energy supply is needed to operate active components.

As an essential example, we consider the Operational Amplifier (OP-AMP). The OP-AMP is a multi-stage, high gain and galvanically coupled differential amplifier. It is used to amplify an electrical signal, and its function is primarily determined by its surrounding circuit. Namely filters can be realized by using OP-AMPs.

Normally OP-AMPs are connected to symmetric operating voltages. But when used with digital circuits, a single voltage supply is preferred. For this case, single supply voltage OP-AMPs are used. Furthermore, rail-to-rail OP-AMPs are have the capability to control the output between the the positive and negative supply voltage.

2.4.3 Applictions

Electrical signal conditioning is based on arrangements of active and passive components in circuits. A good and in depth coverage of active filters and measurement circuits can be found in **Tietze2008**.

3

Data Acquisition and Software

3.1 Data acquistion

The DAC system developed in this thesis is an open source Arduino based system consisting of multiple microcontrollers. All signal channels are transmitted to a central microcontroller before passing to a computer that serves as visualization and analysis tool.

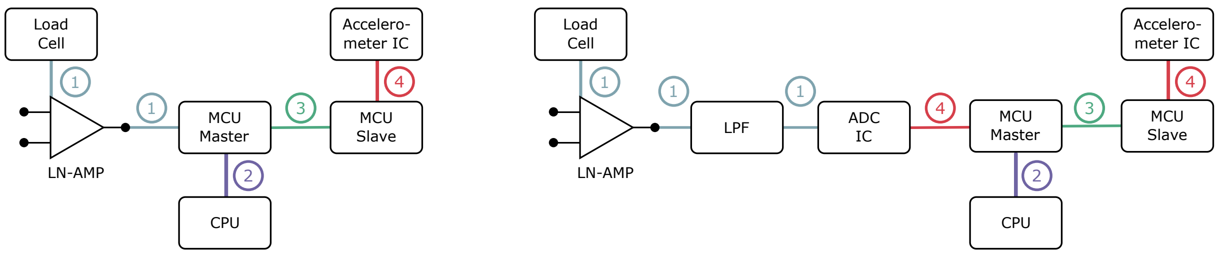

(a) *Without signal conditioning*

(b) *With signal conditioning and external ADC*

Figure 3.1: *DAC-system building blocks – note that 3.1a has been realized, but 3.1b has not been implemented yet, due to communication issues between the devices*

3.1.1 Building Blocks

Building blocks are the main components used in the DAC signal chain. Additional components that are required to enable the stable operation of the building blocks are not listed.

Because the of accelerometer Integrated Circuit (IC) output interfaces it is not possible to connect all sensors directly to one Microcontroller Unit (MCU) that acts as a DAC. We need to transform the signal to a different interface. A low-cost and versatile method to achieve this, is to use a MCU for each

Interfaces	
1	: Analog Signal
2	: Universal Serial Bus (USB)
3	: Recommended Standard (RS)-485
4	: Serial Peripheral Interface (SPI)

Table 3.1: *Legend to Figure 3.1*

accelerometer IC. These read the sensor IC registers and communicate to the MCU master. The master, on the other hand, acts as a passthrough and transmits the data to the Central Processing Unit (CPU). In the setup used, it also reads out the LC signal. Table 3.2 lists the MCUs used during this thesis.

The analog signal output of the LC needs to be amplified to match the input range of the ADC. To gain the maximum resolution, this depends on the expected input range. To get a higher value resolution than offered by the MCU embedded ADC one can set in an external ADC IC upstream to the MCU. Additionally, we use a Low Pass Filter (LPF) in Figure 3.1b. The LPF is needed to cut off high frequency components of the signal that occur particularly in sharp impulse signals. This design choice may lead to problems because it is not standard procedure in the development a measurement instrument. Typically, components in the analog signal chain are chosen, based on the frequency bandwidth of the input signal. This means, the cut-off frequency of the LPF is set well above the signal's bandwidth. But because we use low-cost components in our system, the bandwidth is limited to half the sampling rate of the slowest sensor. According to the Nyquist frequency theorem, the cut-off frequency then needs to be reduced to half the sampling frequency, potentially reducing the output magnitude of higher frequency components of the signal.

Name	Core	ADC-Resolution / bit	Operating Voltage / V	Clock Speed / MHz	Flash Memory / kByte	SRAM / kByte
Arduino Due	AT91SAM3 ARM Cortex	12	3.3	84	512	96
Teensy 3.2	MK20DX256VLH Cortex-M4	13 (16 bit-values)	3.3	72	256	64
Robotdyn Blackpill	STM32F103C8 Cortex-M3	12	72	64	20	

Table 3.2: *List of MCUs used in this work*

3.1.2 Interfaces

The interfaces are the connections and protocols between the different building blocks of the DAC system. The interfaces are chosen based on the sensors used and the expected data rate at the required cable length between each section. I.e.:

- Between the analog LC and the external ADC in Figure 3.1b and the MCU integrated ADC in Figure 3.1a respectively the signal transmission is analog.
- The register of the accelerometer IC is accessed via SPI

- The communication between MCUs is rooted in RS-485 differential transmission to accommodate for signal transmission over cable lengths greater than $10\,\mathrm{m}$ and uses a specialized protocol to keep data packages as small as possible.
- Between the MCU and the CPU USB transmits data using the serial class of the Arduino software.

Data rates and package sizes are critical when sampling at high frequencies.

With RS-485 data can be transmitted over distances of no less than $100\,\mathrm{km}$ at a data rate of $1\,\mathrm{kbit/s}$. At $1200\,\mathrm{m}$ cable length we can reach data rates of around $100\,\mathrm{kbit/s}$. In our range of application, i.e. a few tens of m, we can expect data rates of $1\,\mathrm{Mbit/s}$, thus representing the bottle neck in the digital data chain. If we then transmit $80\,\mathrm{bit}$ acceleration measurements (see Figure 3.2) at $1.6\,\mathrm{kHz}$ we stay below this expected limit by a safety factor of more than 10. The arduino the serial package parses all data as human readable code, specifically American Standard Code For Information Interchange (ASCII). In this format every digit of integer values is passed as $8\,\mathrm{bit}$-value. Which means that a $32\,\mathrm{bit}$ timestamp and every single axis acceleration are passed as ten $8\,\mathrm{bit}$-values and six $8\,\mathrm{bit}$-values respectively. This increases the size of an accelerometer package to $624\,\mathrm{bit}$, which in turn reduces the safety factor to approximately 1. It is clear that one cannot use human readable code to transmit the data and guarantee stability at the required sampling rate.

MCU communication protocol

The communication protocol for MCU to MCU and MCU to computer was developed for this project.

<[(reg) (#bytes) (data)]>

<[/]>	:	Start-/End-bytes, represented as ASCII
(reg)	:	Registry/Address of the transmission
(#Bytes)	:	Number of bytes in transmission
(data)	:	Data to transmit

Table 3.3: *Protocol used to communicate between two MCU's and between MCU and computer*

3.1.3 Dataflow

All MCUs operate sequentially. The dataflow in MCU must be sequential. For this reason during a measurement all data is passed to a central MCU, where it is streamlined to the CPU. The central MCU or master cycles through all connected MCU performing a data request, hold and receive action. As soon as a slave MCU gets a request, it transmits a data package from its buffer. The master now receiving the data package will throughput the signal to the CPU, where it is stored. By the end of this process the master will jump to the next slave.

All measurements consist of a $32\,\mathrm{bit}$-timestamp and the measured values and are pushed into a First In, First Out (FIFO) buffer in the flash memory of the MCU, directly connected to the sensor. Bundled data packages are then pulled from the buffer and translated into the transmission code as defined in Table 3.3. In Figure 3.2 the data flow is represented by a system that is using only one slave MCU, displayed in violet.

Measurements are packaged due to the time the master requires to change the communication to another slave. During these switches no data is transmitted eventually bottlenecking the data rate of the system.

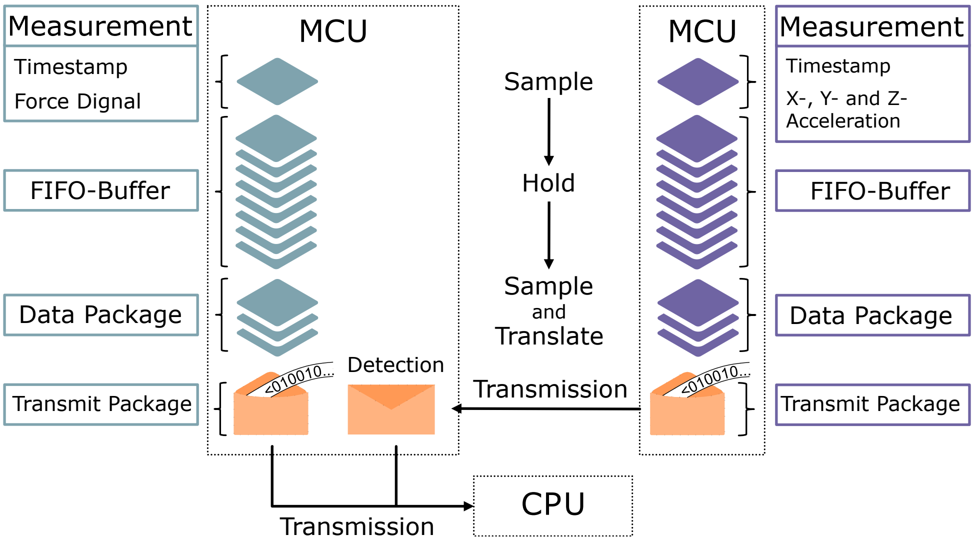

Figure 3.2: *Data flow between two MCUs and the CPU*

3.2 Software

The software developed during this project is split into the Arduino software running on the MCUs and a python based tool to receive and visualize the data via USB.

For the instrument to work, some functions are required, while other desired functions are tools that simplify the workflow during measurements and facilitate bug fixes in the software.

The requirements to the software tools are:

m1 Read out accelerometer and LC data at the maximum sample speed of the accelerometer IC.

m2 Synchronize measurements timestamps.

m3 Initialize measurement by hammer impulse.

The desired software tools are:

w1 Generate continuous real time output of measurement data.

w2 Track data transfer via USB.

4

Test Setups

The test conducted during this thesis isolated features of the prototype system. Measurement data has been compared to a reference system, called MODE3. Both systems are configured to include one impulse hammer, one DAC system and one three dimensional accelerometer, as well as a read out computer system with accompanying software.

4.1 Hammer-Hammer Test

The hammer tips of the impact hammers of both the the prototype system and the MODE3 are hit against each other. The target of this test is to evaluate the signal quality of the LC in the prototype system.

We assume the force transmission from the point of impact to both load cells respectively to be lossless. Thus the recording accuracy of the prototype system is determined by the correlation of the two signal recordings.

The configurations used in the tests are listen in Table 4.1. The components are shown in Figure 4.1. All hammer-hammer tests were conducted, using a DAC of form Figure **??**

Sensor Parameter	Reference Hammer	Prototype Hammer
Sampling rate	1600 Hz	1600 Hz
Dynamic Range	0. . . 20 kN	0. . . 3 kN
Quantization resolution	24 bit	12 bit

Table 4.1: *Hammer-hammer test configuration*

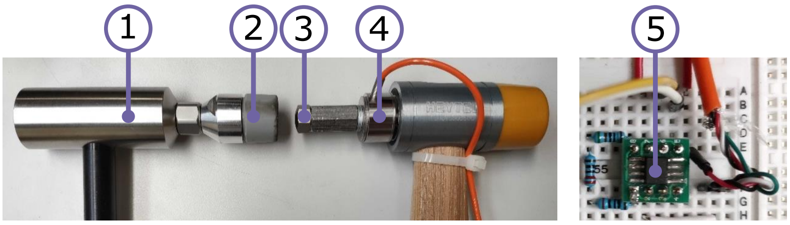

Figure 4.1: *Hammer-Hammer test components*

1	:	Piezo + AMP
2	:	Soft Tip
3	:	Tip 34CrMo4
4	:	LC DYMH-103
5	:	IN-AMP AD627

Table 4.2: *Legend to Figure 4.1*

4.2 Andromeda Measurement

In the Andromeda measurement the accelerometers of both systems are positioned at close locations on the Andromeda test bench. Impact hammers of both the prototype and the reference system may be used as input signal. Because of this, the recording of the accelerometer signal of whichever system's impact hammer is not in use, is initiated before the impact and over a longer time frame. To compare signals of both systems, they are synchronized in the post analysis. The target of this test is to evaluate the signal quality of the accelerometer in the prototype system.

The Andromeda test bench consists of a wagon that is supported by a $3\,\mathrm{m}$ long linear drive in the x-axis on two $2.6\,\mathrm{m}$ apart, gantry y-axes that are linear drives as well. Hence kinematic chain

$$V[b[Y1Y2]X]$$

Figure 4.2 shows the test setup, while Figure 4.3 shows an example position of impact in the test setup.

The focus of this test is to compare the accelerometer signals. Therefore, we set the accelerometer parameter as defined in Table 4.3

Sensor Parameter	Sample Rate / Hz	Dynamic Range / g	Quanti-zation / bit
Reference	1600	± 5	24
Prototype	1600	± 4	16

Table 4.3: *Accelerometer parameter settings*

(a) Andromeda test setup *(b) Accelerometer view*

Figure 4.2: *Andromeda test setup*

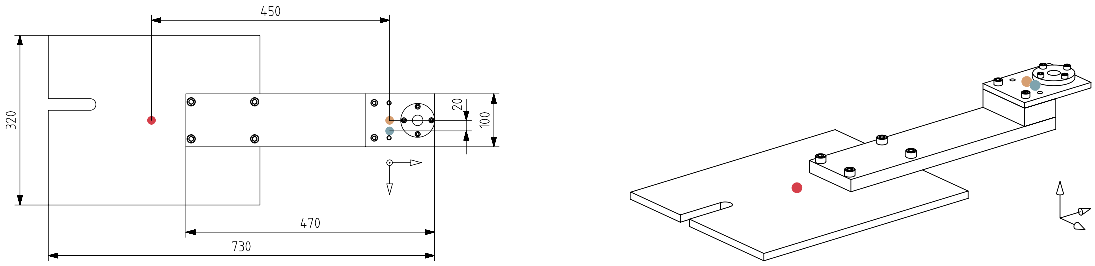

(a) Top view *(b) Trimetric view*

Figure 4.3: *Andromeda wagon, example impact position*

4.3 Other Test Setups

To test the bandwidth of the prototype LC the hammer tip is hit against a rigid surface. The hardness of the hammer tip determines the bandwidth of the signal. And with hard tips the highest bandwidths can be explored. Apart from the signal measurement tests themselves other tests had to be conducted to guarantee the DAC operation and to test the Software. As an example, clock tunable LPF are tested in an arduino circuit, that generates a differential sinusoidal signal at different frequencies.

5

Results and Discussion

In this chapter the results of the setups in **??** are discussed.

5.1 Hammer-Hammer Test

The results of the hammer-hammer test are impulse signal recordings of both, the reference system and the prototype LC. Because the prototype signal is not calibrated, in order to able to compare the signals one needs to normalize the signal range of the reference signal. Furthermore, the signals need to be synced in time, by applying a time shift to one. The outputs gained after these transformations are shown in Figure 5.1.

It can be seen that if one is using the soft PVC tip of the reference system both signals correlate well. If we then focus on the detailed view of such a test, as seen in Figure 5.2, the difference in resolution becomes apparent.

5.2 Andromeda Measurement

Before comparing the accelerometer signals of the reference with the ones of the prototype system, one needs to subtract the constant gravitational part from the prototype signals. Additionally, the signals need to be synchronized in the time axis, as can be seen in Figure 5.3.

When we then consider the frequency domain of Figure 5.4 one can see that both signals cover the excited frequency bandwidth of around $250\,\mathrm{Hz}$ in a similar manner. The initial deviation at $1\,\mathrm{Hz}$ can be explained due to the signal conditioning in the reference system, where lower frequencies are cut-off.

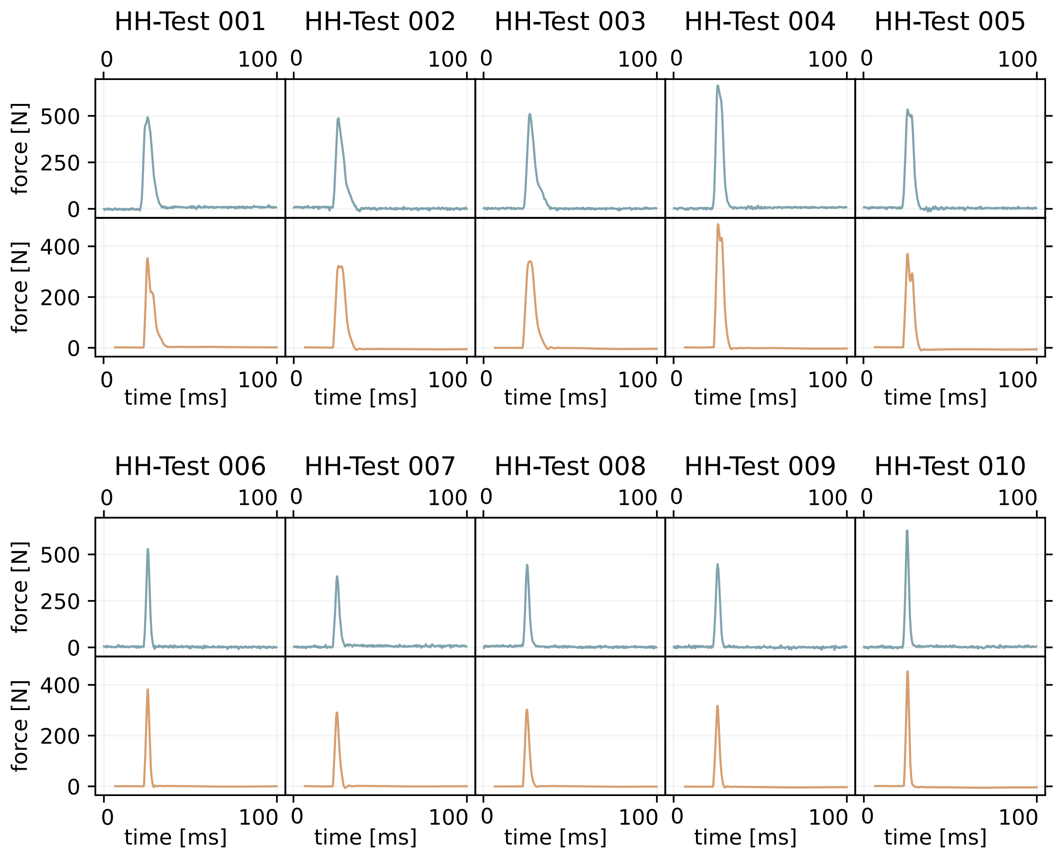

Figure 5.1: *The HH-Test recordings of the reference hammer (orange) and the evaluated impact hammer system (turquoise). Note that the evaluated signal values are normalized so that the maxima are equal to the reference system.*

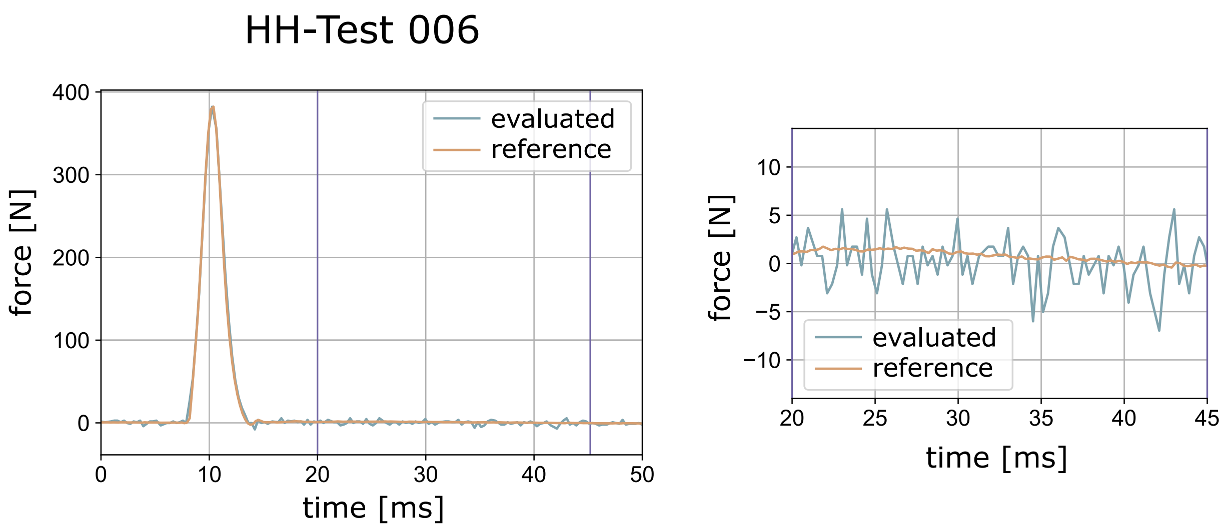

Figure 5.2: *Detailed plot of HH-Test 006*

5.3 Other Test Setups

Other tests failed to deliver results:

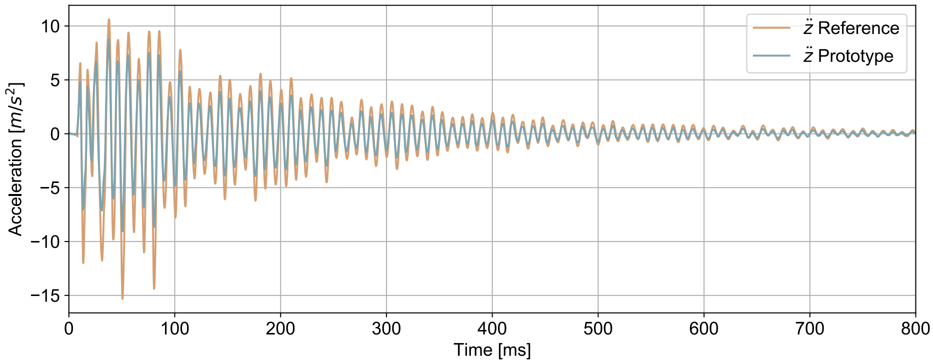

Figure 5.3: *Measurement HAp024 in the time domain, excitation at point A, as shown in Figure 4.3*

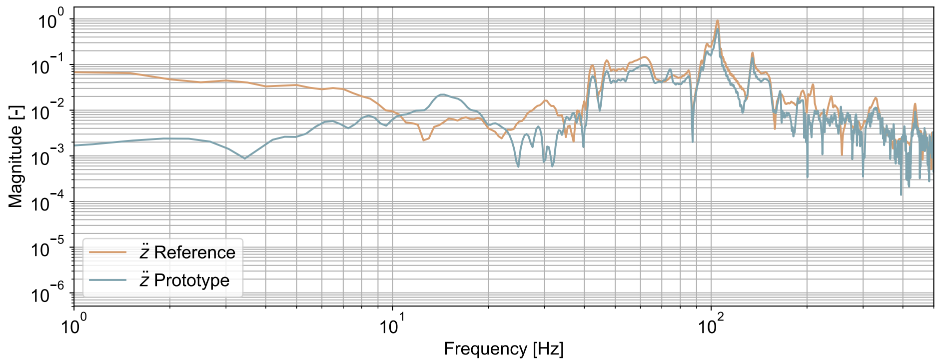

Figure 5.4: *Measurement FFT HAp024, excitation at point A, as shown in Figure 4.3*

- The hammer-surface test did not give insight to the maximum bandwidith of the prototype hammer because of software issues, bottelnecking the data rate.
- The clock tunable filter test failed do to an insufficiently precise clock signal.

6

Conclusion and Future Work

6.1 Conclusion

In this thesis

- A low-cost capacitive accelerometer IC has been used to measure the output signal of an EMA measurement setup
- An impulse hammer using a strain gauge load cell has been developed using low-cost components.
- Different conditioning filter circuits have been studied and tested for the impulse hammer signal
- A communication protocol has been developed

6.1.1 Deficiencies

Because of the lack of a thorough state of the art research in the beginning of the project, the solution space of the project has been constricted early on. In this solution space, the data rates and the required compute efficiency of MCUs were not met by the software. Furthermore, the issue of conditioning the analog signal of the LC signal has been addressed at a late stage. Leading to no successful hardware setup with an upstream LPF.

6.2 Future Work

There are multiple options to progress from this point. They can be framed in ... directions:

- Explore the same solution space further, i.e. handling the LPF circuit and optimizing the software.
- Change to a different solution space with either standard components using CPUs or Field Programmable Gate Array (FPGA)s, targeting simpler implementation or higher bandwidths
- Exploring the limits of the application and limits current solution without additional preconditioning

Independent of the chosen direction one can progress by

- Testing the limits of multi channelling
- Leaving the prototyping stage and simplify the production
- Exploring wireless communication

A

Appendix

Table A.1: *Andromeda measurement setup that is excited by the prototype impact hammer. The prototype accelerometer is set to a dynamic range of* $\pm 16\,\mathrm{g}$ *and a AAF cut-off of* $800\,\mathrm{Hz}$.

Label	Excitation Location	Prototype Sampling Rate / kHz	Prototype Recording Duration / s
HAe001	A	1.6	3
HAe002	A	1.6	3
HAe003	A	1.6	3
HAe004	A	1.6	3
HAe005	A	1.6	3
HAe006	B	1.6	3
HAe007	B	1.6	3
HAe008	B	1.6	3
HAe009	B	1.6	3
HAe010	B	1.6	3
HAe011	C	1.6	3
HAe012	C	1.6	3
HAe013	C	1.6	3
HAe014	C	1.6	3
HAe015	C	1.6	3
HAe016	D	1.6	3
HAe017	D	1.6	3
HAe018	D	1.6	3
HAe019	D	1.6	3

continued on next page

Table A.1: *(Continued)*

Label	Excitation Location	Prototype Sampling Rate / kHz	Prototype Recording Duration / s
HAe020	D	1.6	3

Table A.2: *Andromeda measurement setup that is excited by the reference impact hammer*

Label	Excitation Location	Accelerometer Sampling Rate / kHz	Prototype Recording Duration / s	Accelrometer Dynamic Range / g	Accelerometer AAF cut-off / Hz
HAp001	A	1.6	3	±16	800
HAp002	A	1.6	3	±16	800
HAp003	A	1.6	3	±16	800
HAp004	A	1.6	3	±16	800
HAp005	A	1.6	3	±16	800
HAp006	B	1.6	3	±16	800
HAp007	B	1.6	3	±16	800
HAp008	B	1.6	3	±16	800
HAp009	B	1.6	3	±16	800
HAp010	B	1.6	3	±16	800
HAp011	C	1.6	3	±16	800
HAp012	C	1.6	3	±16	800
HAp013	C	1.6	3	±16	800
HAp014	C	1.6	3	±16	800
HAp015	C	1.6	3	±16	800
HAp016	D	1.6	3	±16	800
HAp017	D	1.6	3	±16	800
HAp018	D	1.6	3	±16	800
HAp019	D	1.6	3	±16	800
HAp020	D	1.6	3	±16	800
HAp001	A	0.8	3	±16	400
HAp002	A	0.8	3	±16	400
HAp003	A	0.8	3	±16	400
HAp004	A	0.8	3	±16	400
HAp005	A	0.8	3	±16	400
HAp006	B	0.8	3	±16	400
HAp007	B	0.8	3	±16	400
HAp008	B	0.8	3	±16	400
HAp009	B	0.8	3	±16	400
HAp010	B	0.8	3	±16	400
HAp011	C	0.8	3	±16	400
HAp012	C	0.8	3	±16	400
HAp013	C	0.8	3	±16	400
HAp014	C	0.8	3	±16	400

continued on next page

Table A.2: *(Continued)*

Label	Excitation Location	Accelerometer Sampling Rate / kHz	Prototype Recording Duration / s	Accelrometer Dynamic Range / g	Accelerometer AAF cut-off / Hz
HAp015	C	0.8	3	± 16	400
HAp016	D	0.8	3	± 16	400
HAp017	D	0.8	3	± 16	400
HAp018	D	0.8	3	± 16	400
HAp019	D	0.8	3	± 16	400
HAp020	D	0.8	3	± 16	400
HAp021	C	1.6	3	± 4	800
HAp022	C	1.6	3	± 4	800
HAp023	C	1.6	3	± 4	800
HAp024	C	1.6	3	± 4	800
HAp025	C	1.6	3	± 4	800
HAp026	D	1.6	3	± 2	800
HAp027	D	1.6	3	± 2	800
HAp028	D	1.6	3	± 4	800
HAp029	D	1.6	3	± 4	800
HAp030	D	1.6	3	± 4	800

Table A.3: *Hammer-hammer test measurements*

Label	Prototype tip	Prototype Sampling Rate / kHz	Prototype Recording Duration / s
HH001	34CrMo4	3	4
HH002	34CrMo4	3	4
HH003	34CrMo4	3	4
HH004	34CrMo4	3	4
HH005	34CrMo4	3	4
HH006	34CrMo4	3	4
HH007	34CrMo4	3	4
HH008	34CrMo4	3	4
HH009	34CrMo4	3	4
HH010	34CrMo4	3	4
HH011	34CrMo4	3	3
HH012	34CrMo4	2	3
HH013	34CrMo4	2	3
HH014	34CrMo4	2	3
HH015	34CrMo4	2	3
HH016	Elastomer	2	3
HH017	Elastomer	2	3
HH018	Elastomer	2	3
HH019	Elastomer	2	3

continued on next page

Table A.3: *(Continued)*

Label	Prototype tip	Prototype Sampling Rate / kHz	Prototype Recording Duration / s
HH020	Elastomer	2	3

Table A.4: *Hammer-surface measurements*

Label	Prototype tip	Prototype Sampling Rate / kHz	Prototype Recording Duration / s
HS001	34CrMo4	2	1
HS002	34CrMo4	2	1
HS003	34CrMo4	2	1
HS004	34CrMo4	2	1
HS005	34CrMo4	2	1
HS006	34CrMo4	2.5	1
HS007	34CrMo4	2.5	1
HS008	34CrMo4	2.5	1
HS009	34CrMo4	2.5	1
HS010	34CrMo4	2.5	1
HS011	34CrMo4	1.67	1
HS012	34CrMo4	1.67	1
HS013	34CrMo4	1.67	1
HS014	34CrMo4	1.67	1
HS015	34CrMo4	1.67	1
HS016	Elastomer	1.67	1
HS017	Elastomer	1.67	1
HS018	Elastomer	1.67	1
HS019	Elastomer	1.67	1
HS020	Elastomer	1.67	1
HS021	Elastomer	2	1
HS022	Elastomer	2	1
HS023	Elastomer	2	1
HS024	Elastomer	2	1
HS025	Elastomer	2	1
HS026	Elastomer	2.5	1
HS027	Elastomer	2.5	1
HS028	Elastomer	2.5	1
HS029	Elastomer	2.5	1
HS030	Elastomer	2.5	1

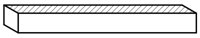

(a) *Vertical stress, longitudinal particle displacement*

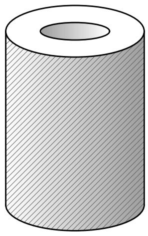

(d) *Lateral stress, lateral particle displacement*

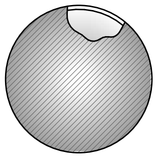

(g) *Vertical stress, radial particle displacement*

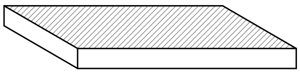

(b) *Vertical stress, lateral particle displacement*

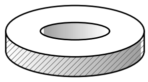

(e) *Radial particle displacement*

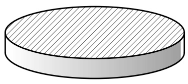

(h) *Radial particle displacement*

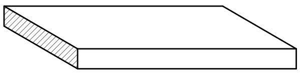

(c) *Vertical stress, lateral particle displacement*

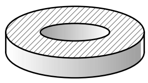

(f) *Radial particle displacement*

(i) *Radial particle displacement*

Figure A.1: *Piezoelectric designs, where electrodes are placed on the shaded areas*

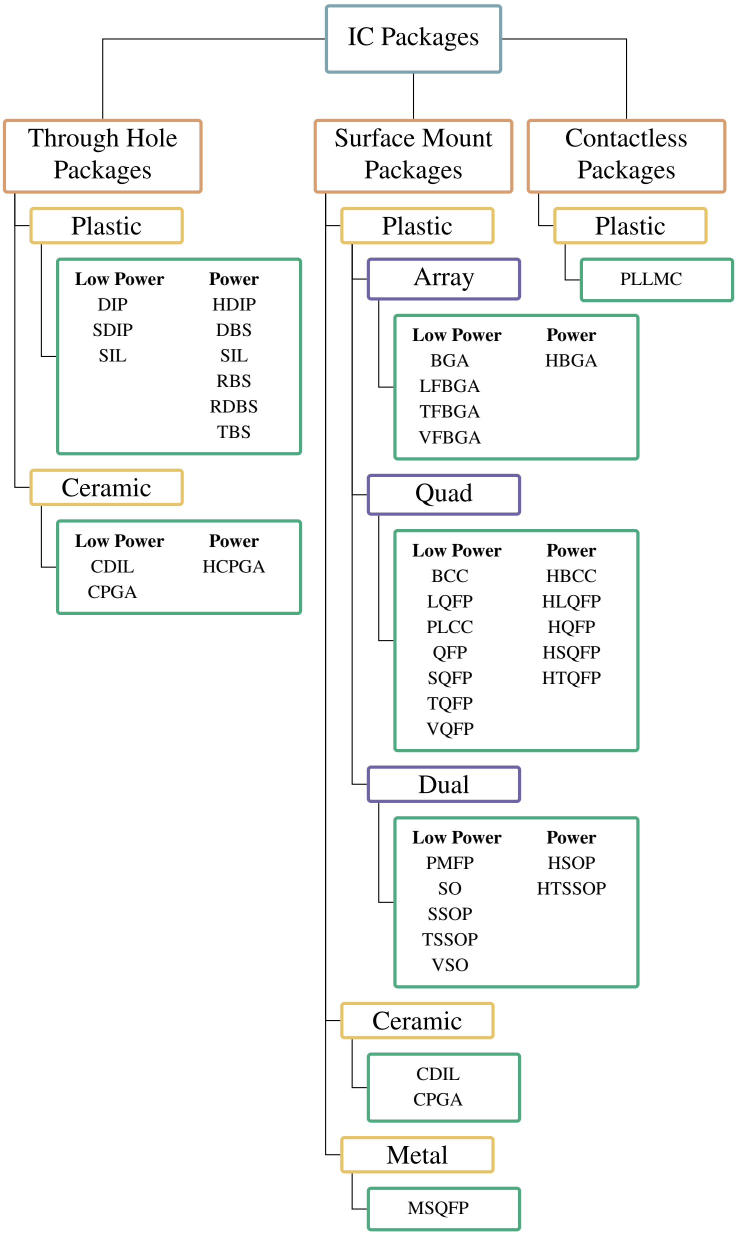

Figure A.2: *Flowchart of IC packages [9]*

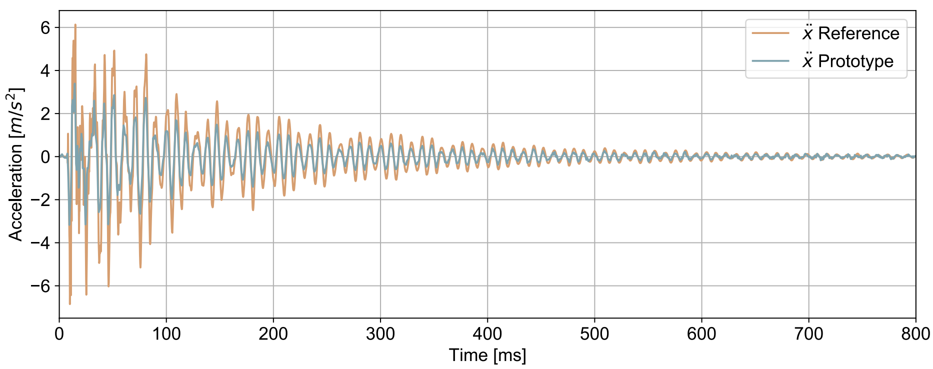

Figure A.3: *Measurement HAp024 in the time domain, excitation at point A, as shown in Figure 4.3*

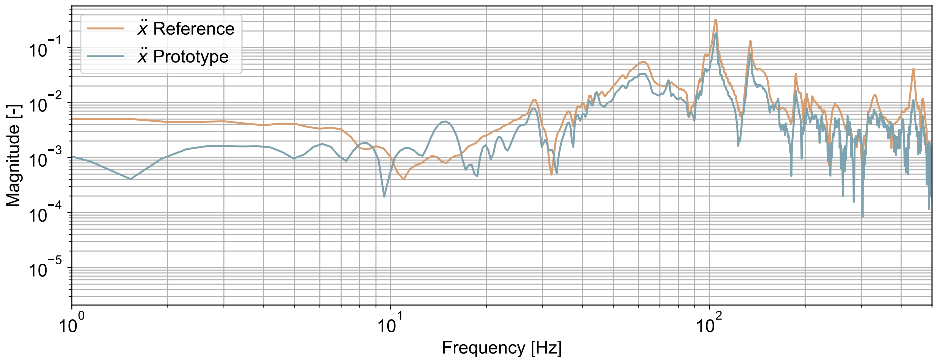

Figure A.4: *Measurement FFT HAp024, excitation at point A, as shown in Figure 4.3*

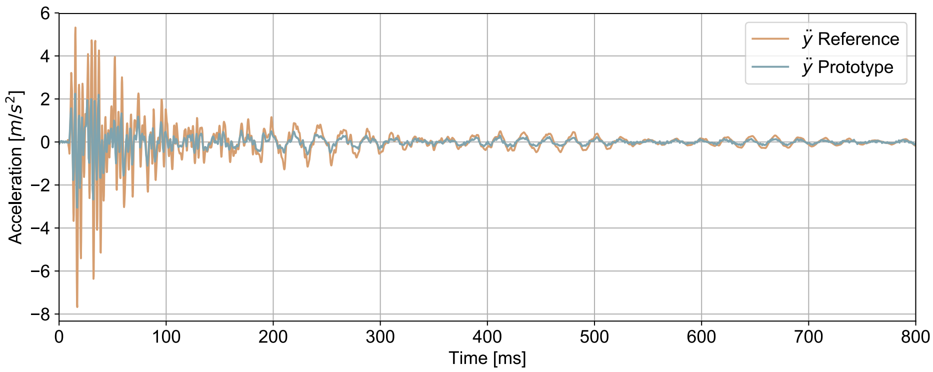

Figure A.5: *Measurement HAp024 in the time domain, excitation at point A, as shown in Figure 4.3*

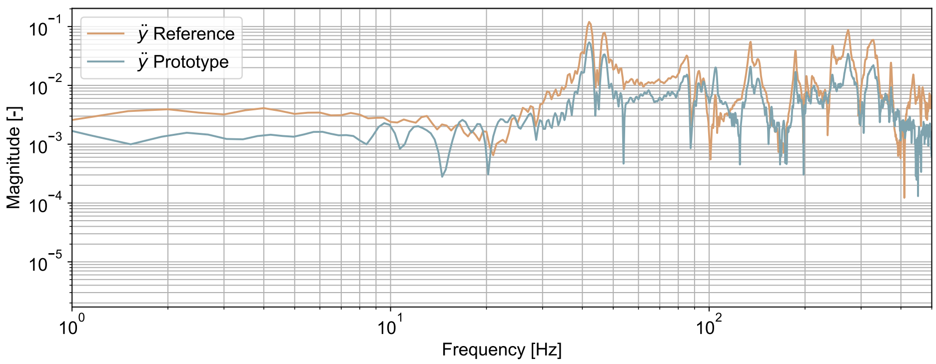

Figure A.6: *Measurement FFT HAp024, excitation at point A, as shown in Figure 4.3*

List of Figures

List of Tables

Bibliography

[1] Sherif Beskhyroun and Q. Ma. “Low-cost accelerometers for experimental modal analysis”. In: *Proc. of the 15th World Conference on Earthquake Engineering*. 2012.

[2] Yum Ji Chan and Jing-Wei Huang. “Multiple-point vibration testing with micro-electromechanical accelerometers and micro-controller unit”. In: *Mechatronics* 44 (2017), pp. 84–93.

[3] Ozak O Esu et al. “Integration of low-cost consumer electronics for in-situ condition monitoring of wind turbine blades”. In: (2014).

[4] Zhi-Fang Fu and Jimin He. *Modal analysis*. Elsevier, 2001.

[5] Alberto Girolami et al. “Modal analysis of structures with low-cost embedded systems”. In: *2018 IEEE International Symposium on Circuits and Systems (ISCAS)*. IEEE. 2018, pp. 1–4.

[6] Gianfranco Piana et al. “Experimental modal analysis of straight and curved slender beams by piezoelectric transducers”. In: *Meccanica* 51.11 (2016), pp. 2797–2811.

[7] Brian J Schwarz and Mark H Richardson. “Experimental modal analysis”. In: *CSI Reliability week* 35.1 (1999), pp. 1–12.

[8] Stiny. *Aktive elektronische Bauelemente*. Springer Fachmedien Wiesbaden, 2019.

[9] Tietze. *Electronic Circuits*. Springer Berlin Heidelberg, 2008.

[10] Josef Vollmer et al. “Construction kit for low-cost vibration analysis systems based on low-cost acceleration sensors”. In: *2009 IEEE/ASME International Conference on Advanced Intelligent Mechatronics*. IEEE. 2009, pp. 463–468.

[11] Chris Waltham and Andrzej Kotlicki. “Construction and calibration of an impact hammer”. In: *American Journal of Physics* 77.10 (2009), pp. 945–949.

[12] Tong Wang et al. “Practical calibration techniques for the modal impact hammer”. In: *Sensors and Instrumentation, Volume 5*. Springer, 2015, pp. 23–29.

[13] John G Webster and Halit Eren. *Measurement, Instrumentation, and Sensors Handbook: Two-Volume Set*. CRC press, 2018.